Interaction of CO_2 concentrations and water stress in semi-arid plants causes diverging response in instantaneous water use efficiency and carbon isotope composition

Na Zhao[1,3], Ping Meng[2], Yabing He[1], Xinxiao Yu[1,3]*

[1] College of soil and water conservation, Beijing Forestry University, Beijing 100083, P.R. China
[2] Research Institute of Forestry, Chinese Academy of Forestry 100091, Beijing, P.R. China
[3] Beijing collaborative innovation center for eco-environmental improvement with forestry and fruit trees

Abstract. In the context of global warming attributable to the increasing levels of CO_2, severe drought may be more frequent in areas with chronic water shortages (semi-arid areas). This necessitates research on the interactions between increased levels of CO_2 and drought on plant photosynthesis. It is commonly reported that ^{13}C fractionation occurs as CO_2-gas diffuses from the atmosphere to the sub-stomatal cavity. Few researchers have investigated ^{13}C fractionation at the site of carboxylation to cytoplasm before sugars are exported outward from the leaf. This process typically progresses in response to variations in environmental conditions (i.e., CO_2 concentrations and water stress), including in their interaction. Therefore, saplings of two typical plant species (*Platycladus orientalis* and *Quercus variabilis*) from semi-arid areas of Northern China were selected and cultivated in growth chambers with orthogonal treatments (four CO_2 concentration ($[CO_2]$) × five soil volumetric water content (SWC)). The $\delta^{13}C$ of water-soluble compounds extracted from leaves of saplings was determined for an assessment of instantaneous water use efficiency (WUE_{cp}) after cultivation. Instantaneous water use efficiency derived from gas-exchange measurement (WUE_{ge}) was integrated to estimate differences in $\delta^{13}C$ signal variation before leaf-level translocation of primary assimilates. The WUE_{ge} in *P. orientalis* and *Q. variabilis* both decreased with increased soil moisture at 35–80% of field capacity (FC), and increased with elevated $[CO_2]$ by increasing photosynthetic capacity and reducing transpiration. Instantaneous water use efficiency (iWUE) according to environmental changes, differed between the two species. The WUE_{ge} in *P. orientalis* was significantly greater than that in *Q. variabilis*, while an opposite tendency was observed when comparing WUE_{cp} between the two species. Total ^{13}C fractionation at the site of carboxylation to cytoplasm before sugar export (total ^{13}C fractionation) was species-specific, as demonstrated in the interaction of $[CO_2]$ and SWC. Rising $[CO_2]$ coupled with moistened soil generated increasing disparities in $\delta^{13}C$ between water-soluble compounds ($\delta^{13}C_{WSC}$) and estimates based on gas-exchange observations ($\delta^{13}C_{obs}$) in *P. orientalis*, ranging between 0.0328–0.0472‰. Differences between $\delta^{13}C_{WSC}$ and $\delta^{13}C_{obs}$ in *Q. variabilis* increased as $[CO_2]$ and SWC increased (0.0384–0.0466‰). The ^{13}C fractionation from mesophyll conductance (g_m) and post-carboxylation both contributed to the total ^{13}C fractionation that was determined by $\delta^{13}C$ of water-soluble compounds and gas-exchange measurements. Total ^{13}C fractionation was linearly dependent on stomatal conductance, indicating post-carboxylation fractionation could be attributed to environmental variation. The magnitude and environmental dependence of apparent post-carboxylation fractionation is worth our attention when addressing photosynthetic fractionation.

Key words: Post-carboxylation fractionation; Carbon isotope fractionation; Elevated CO_2 concentration; Soil volumetric water content; Instantaneous water use efficiency

1 Introduction

Since the industrial revolution, atmospheric CO_2 concentration has increased at an annual rate of 0.4%, and is expected to increase to 700 μmol·mol^{-1}, culminating in more frequent periods of dryness (IPCC, 2014). Increasing atmospheric CO_2 concentrations that exacerbate the greenhouse effect will increase fluctuations in global precipitation patterns, which will probably amplify drought frequency in arid regions and lead to more frequent extreme flooding events in humid regions (Lobell et al., 2014). Accompanying the increasing concentration of CO_2, mean $\delta^{13}C$ of atmospheric CO_2 is currently being depleted by 0.02‰–0.03‰ year^{-1} (CU-INSTAAR/NOAACMDL network for atmospheric CO_2; http://www.esrl.noaa.gov/gmd/).

The current carbon isotopic composition may respond to environmental change and its influence on diffusion via plant physiological and metabolic processes (Gessler et al., 2014; Streit et al., 2013). While depletion of $\delta^{13}C_{CO_2}$ is occurring in the atmosphere, variations in CO_2 concentration ($[CO_2]$) may affect $\delta^{13}C$ of plant organs which, in turn, respond physiologically to changes in climate (Gessler et al., 2014). The carbon discrimination ($^{13}\Delta$) in leaves could also provide timely feedback to the availability of soil moisture and atmospheric vapor pressure deficit (Cernusak et al., 2012). Discrimination of ^{13}C in leaves relies mainly on environmental factors that affect the ratio of intercellular to ambient $[CO_2]$ (C_i/C_a). Rubisco activities and the mesophyll conductance derived from the difference of $[CO_2]$ between intercellular sites and chloroplasts are also involved (Farquhar et al., 1982; Cano et al., 2014). Changes in environmental conditions affect photosynthetic discrimination, recording differentially in the $\delta^{13}C$ of water-soluble compounds ($\delta^{13}C_{WSC}$) in different plant organs. Several processes during photosynthesis alter the $\delta^{13}C$ of carbon transported within plants. Carbon-fractionation during photosynthetic CO_2 fixation has been reviewed elsewhere (Farquhar et al., 1982; Farquhar and Sharkey, 1982).

Post-photosynthetic fractionation is derived from equilibrium and kinetic isotopic effects that determine isotopic differences between metabolites and intramolecular reaction positions. These are defined as "post-photosynthetic" or "post-carboxylation" fractionation (Jäggi et al., 2002; Badeck et al., 2005; Gessler et al., 2008). Post-carboxylation fractionation in plants includes the carbon discrimination that follows carboxylation of ribulose-1, 5-bisphosphate and internal diffusion (RuBP, 27‰), as well as related transitory starch metabolism (Gessler et al., 2008; Gessler et al., 2014), fractionation-associated phloem transport, remobilization or storage of soluble carbohydrates, and starch metabolism fractionation in sink tissue (tree rings). In the synthesis of soluble sugars, ^{13}C-depletions of triose phosphates occur during export from the cytoplasm, and during production of fructose-1, as does 6-bisphosphate by aldolase in transitory starch synthesis (Rossmann et al., 1991; Gleixner and Schmidt, 1997). Synthesis of sugars before transportation to the twig is associated with the post-carboxylation fractionation generated in leaves. Although these are likely to play a role, another consideration is $[CO_2]$ in the chloroplast (C_c), not in the intercellular space, as considered in the simplified equation of Farquhar's model (Evans et al., 1986; Farquhar et al., 1989) is actually defined as carbon isotope discrimination ($\delta^{13}C$). Differences between gas-exchange derived values and online measurements of $\delta^{13}C$ have often been used to estimate C_i-C_c and mesophyll conductance for CO_2 (Le Roux et al., 2001; Warren and Adams, 2006; Flexas et al., 2006; Evans et al., 2009; Flexas et al., 2012; Evans and von Caemmerer 2013). In this regard, changes in mesophyll conductance could be partly responsible for the differences in the two measurements, as it generally increases in the short term in response to elevated

CO_2 (Flexas et al., 2014), but tends to decrease under drought (Hommel et al., 2014; Théroux-Rancourt et al., 2014). Therefore, it is necessary to avoid confusion between carbon isotope discrimination derived from synthesis of soluble sugars and/or mesophyll conductance. The degree to which carbon fractionation is related to environmental variation has yet to be fully investigated.

The simultaneous isotopic analysis of leaves allows determination of temporal variation in isotopic fractionation (Rinne et al., 2016). This will aid in the accurate recording of environmental conditions. Newly assimilated carbohydrates can be extracted, and these are termed the water-soluble compounds (WSCs) in leaves (Brandes et al., 2006; Gessler et al., 2009). WSCs can also be associated with an assimilation-weighted mean of C_i/C_a (and C_c/C_a) photosynthesized over periods ranging from a few hours to 1–2 days (Pons et al., 2009). However, there is disagreement whether fractionation caused by post-carboxylation and/or mesophyll resistance can alter the stable signatures of leaf carbon and thence influence instantaneous water use efficiency (iWUE). In addition, the manner in which iWUE derived from isotopic fractionation responds to environmental factors, such as elevated $[CO_2]$ and/or soil water gradients, is unknown.

Consequently, we investigated the $\delta^{13}C$ of the fast-turnover carbohydrate pool in sapling leaves of two tree species, *Platycladus orientalis* (L.) Franco and *Quercus variabilis* Bl., native to semi-arid areas of China. We conducted gas-exchange measurements in controlled-environment growth chambers. One goal is to differentiate the ^{13}C fractionation from the site of carboxylation to cytoplasm prior to sugar transportation in *P. orientalis* and *Q. variabilis*, which is the total ^{13}C fractionation determined from the $\delta^{13}C$ of WSCs and gas-exchange measurements. Another goal is to discuss the potential causes for the observed divergence, estimate contributions of post-photosynthesis and mesophyll conductance on these differences, and describe how carbon isotopic fractionation responds to the interactive effects of elevated $[CO_2]$ and water stress.

2 Material and Methods

2.1 Study site and design

P. orientalis and *Q. variabilis* saplings, selected as experimental material, were obtained from the Capital Circle forest ecosystem station, a part of Chinese Forest Ecosystem Research Network (CFERN), 40°03'45"N, 116°5'45"E, Beijing, China. This region is forested by *P. orientalis* and *Q. variabilis*. We chose saplings of similar basal diameters, heights, and growth class. Each sapling was placed into an individual pot (22 cm diam. × 22 cm high). Undisturbed soil samples were collected from the field, sieved (with particles >10 mm removed), and placed into the pots. The soil bulk density in the pots was maintained at 1.337–1.447 $g \cdot cm^{-3}$. After a 30-day transplant recovery period, the saplings were placed into growth chambers for orthogonal cultivation.

The controlled experiment was conducted in growth chambers (FH-230, Taiwan Hipoint Corporation, Kaohsiung City, Taiwan). To reproduce the meteorological conditions of different growing seasons in the research region, daytime and nighttime temperatures in the chambers were set to 25 ± 0.5℃ from 07:00 to 17:00 and 18 ± 0.5℃ from 17:00 to 07:00. Relative humidity was maintained at 60% and 80% during the daytime and nighttime, respectively. The mean daytime light intensity was 200–240 $\mu mol \cdot m^{-2} \cdot s^{-1}$. The chamber system was designed to control and monitor $[CO_2]$. Two growth chambers (A and B) were used in this study. Chamber A maintained $[CO_2]$ at 400 ppm (C_{400}) and 500 ppm (C_{500}). Chamber B maintained $[CO_2]$ at 600 ppm (C_{600}) and 800 ppm (C_{600}). The target $[CO_2]$ in each chamber had a standard deviation of ± 50 ppm during plant cultivation and testing.

An automatic watering device was used to irrigate the potted saplings to avoid heterogeneity when scheduled watering was not made (Fig. 1). The watering device consisted of a water storage tank, holder, controller, soil moisture sensors, and a drip irrigation component. Prior to use, the tank was filled with water, and the soil moisture sensor was inserted to a uniform depth in the soil. After connecting the controller to an AC power supply, target soil volumetric water content (SWC) could be set and monitored by soil moisture sensors. Since changes in SWC could be sensed by the sensors, this automatic watering device could be regulated to begin ~~watering~~ or stop watering the plants. One irrigation device was installed per chamber. Based on mean field capacity (FC) of potted soil (30.70%), we established orthogonal treatments of four [CO_2] × five SWC (Table. 1). In Table 1, A_1-A_4 denotes [CO_2] of 400 (C_{400}), 500 (C_{500}), 600 (C_{600}) and 800 ppm (C_{800}) in the chambers; B_1-B_5 denotes 35–45% (10.74–13.81%), 50–60% (15.35–18.42%), 60–70% (18.42–21.49%), 70–80% (21.49–24.56%), and 100% of FC (CK, 27.63–30.70%). Each orthogonal treatment of [CO_2] × SWC for two saplings per species was repeated twice. Each treatment lasted 7 days. One pot was exposed in each of the [CO_2] × SWC treatments. Pots in the chambers were rearranged every two days to promote uniform illumination.

2.2 Foliar gas exchange measurement

Fully expanded primary annual leaves of the saplings were measured with a portable infrared gas photosynthesis system (LI-6400, Li-Cor, Lincoln, US) before and after the 7-day cultivation. Two saplings per species were replicated per treatment (SWC× [CO_2]). For each sapling, four leaves were sampled and four measurements were conducted on each leaf. Main photosynthetic parameters, such as net photosynthetic rate (P_n) and transpiration rate (T_r), were measured. Based on theoretical considerations of Von Caemmerer and Farquhar (1981), stomatal conductance (g_s) and intercellular [CO_2] (C_i) were calculated by the Li-Cor software. Instantaneous water use efficiency via gas exchange (WUE_{ge}) was calculated as the ratio P_n / T_r.

2.3 Plant material collection and leaf water-soluble compounds extraction

Eight recently-expanded sun leaves were selected per sapling and homogenized in liquid nitrogen after gas-exchange measurements were finished. For extraction of WSCs from the leaves (Gessler et al., 2004), 50 mg of ground leaves and 100 mg of PVPP (polyvinylpolypyrrolidone) were mixed and incubated in 1 mL distilled water for 60 min at 5℃ in a centrifuge tube. Each leaf sample was replicated twice. The tubes containing the mixture were heated in 100℃ water for 3 min. After cooling to room temperature, the supernatant of the mixture was centrifuged (12000 × g for 5 min) and 10 μL of supernatant was transferred into a tin capsule and dried at 70℃. Folded capsules were used for $\delta^{13}C$ analysis of WSCs. The samples of WSCs from leaves were combusted in an elemental analyzer (EuroEA, HEKAtech GmbH, Wegberg, Germany) and analyzed with a mass-spectrometer (DELTA^{plus}XP, ThernoFinnigan).

Carbon isotope signatures were expressed in δ-notation (parts per thousand), relative to the international Pee Dee Belemnite (PDB) standard:

$$\delta^{13}C = \left(\frac{R_{sample}}{R_{standard}} - 1\right) \times 1000 \quad (1)$$

where $\delta^{13}C$ is the heavy isotope and R_{sample} and $R_{standard}$ refer to the isotope ratio between the particular substance and the corresponding standard, respectively. The precision of repeated measurements was 0.1 ‰.

2.4 Isotopic calculation

2.4.1 ^{13}C fractionation from the site of carboxylation to cytoplasm prior to sugar transportation

Based on the linear model of Farquhar and Sharkey (1982), the isotope discrimination, Δ, was calculated as

$$\Delta = (\delta^{13}C_a - \delta^{13}C_{WSC})/(1 + \delta^{13}C_{WSC}), \quad (2)$$

where $\delta^{13}C_a$ and $\delta^{13}C_{WSC}$ are the isotope signatures of ambient [CO_2] in chambers and WSCs extracted from leaves, respectively. The C_i:C_a was determined by

$$C_i: C_a = (\Delta - a)/(b - a), \quad (3)$$

where C_i and C_a are the [CO_2] within substomatal cavities and in growth chambers, respectively; a is the fractionation occurring CO_2 diffusion in still air (4‰) and b refers to the discrimination during CO_2 fixation by ribulose 1,5- bisphosphate carboxylase/oxygenase (Rubisco) and internal diffusion (30‰). Instantaneous water use efficiency by gas-exchange measurement (WUE_{ge}) was calculated as

$$WUE_{ge} = P_n: T_r = (C_a - C_i)/1.6\Delta e, \quad (4)$$

where 1.6 is the diffusion ratio of stomatal conductance for water vapor to CO_2 in chambers and Δe is the difference between e_{lf} and e_{atm}, representing the extra- and intra-cellular water vapor pressure, respectively:

$$\Delta e = e_{lf} - e_{atm} = 0.611 \times e^{17.502T/(240.97+T)} \times (1 - RH), \quad (5)$$

where T and RH are the leaf-surface temperature and relative humidity, respectively. Combining Eqns. (2, 3 and 4), the instantaneous water use efficiency was determined by the $\delta^{13}C_{WSC}$ of leaves, defined as:

$$WUE_{cp} = \frac{P_n}{T_r} = (1 - \varphi)(C_a - C_i)/1.6\Delta e = C_a(1 - \varphi)\left[\frac{b-\delta^{13}C_a+(b+1)\delta^{13}C_{WSC}}{(b-a)(1+\delta^{13}C_{WSC})}\right]/1.6\Delta e, \quad (6)$$

where φ is the respiratory ratio of leaf carbohydrates to other organs at night (0.3).

Then the ^{13}C fractionation from the site of carboxylation to cytoplasm prior to sugar transportation (defined as the total ^{13}C fractionation) was estimated by the observed $\delta^{13}C$ of WSCs from leaves ($\delta^{13}C_{WSC}$) and the modeled $\delta^{13}C$ calculated from gas-exchange measurements ($\delta^{13}C_{model}$). The $\delta^{13}C_{model}$ was calculated by Δ_{model} from Eqn. (2); Δ_{model} was determined by combining Eqns. (3 and 4) as

$$\Delta_{model} = (b - a)\left(1 - \frac{1.6\Delta e WUE_{ge}}{C_a}\right) + a, \quad (7)$$

$$\delta^{13}C_{model} = \frac{C_a - \Delta_{model}}{1 + \Delta_{model}}, \quad (8)$$

$$\text{Total } ^{13}C \text{ fractionation} = \delta^{13}C_{WSC} - \delta^{13}C_{model}. \quad (9)$$

2.4.2 Method of estimating mesophyll conductance and the contribution of post-carboxylation fractionation

CO_2 diffusion into photosynthetic sites includes two main processes. CO_2 first moves from ambient air surrounding the leaf (C_a) through stomata to the sub-stomatic cavities (C_i). From sub-stomatic cavities, CO_2 then moves to the sites of carboxylation within the chloroplast stroma (C_c) of the leaf mesophyll. The latter procedure of diffusion is termed mesophyll conductance (g_m; Flexas et al., 2008). The carbon isotope discrimination was generated from the relative contribution of diffusion and carboxylation, reflected by C_c to C_a. The carbon isotopic discrimination (Δ) can be presented as (Farquhar et al. 1982):

$$\Delta = a_b \frac{C_a - C_s}{C_a} + a \frac{C_s - C_i}{C_a} + (e_s + a_l) \frac{C_i - C_c}{C_a} + b \frac{C_c}{C_a} - \frac{\frac{eR_D}{k} + f\Gamma_*}{C_a}, \quad (10)$$

where C_a, C_s, C_i, and C_c are the [CO_2] in the ambient air, at the boundary layer of the leaf, in the substomatal cavities, and at the sites of carboxylation, respectively; a_b is the CO_2 diffusional fractionation at the boundary layer (2.9‰); e_s is the discrimination for CO_2 diffusion when CO_2 enters in solution (1.1‰, at 25℃); a_l is the CO_2 diffusional fractionation in the liquid phase (0.7‰); e and f are carbon discriminations derived in dark respiration (R_D) and photorespiration, respectively; k is the carboxylation efficiency, and Γ^* is the CO_2 compensation point in the absence of dark respiration (Brooks and Farquhar,1985).

When gas in the cuvette is well stirred during gas-exchange measurements, diffusion across the boundary layer could be neglected and Eqn. (10) can be written as

$$\Delta = a \frac{C_a - C_i}{C_a} + (e_s + a_l) \frac{C_i - C_c}{C_a} + b \frac{C_c}{C_a} - \frac{\frac{eR_D}{k} + f\Gamma_*}{C_a}. \quad (11)$$

There is no consensus about the value of e, although recent measurements estimate it as ranging from 0-4‰. The value of f has been estimated to range from 8-12‰ (Gillon and Griffiths, 1997; Igamberdiev et al., 2004; Lanigan et al., 2008). As the most direct factor, b influences the calculation of g_m, which is thought to be approximately 30‰ in higher plants (Guy et al., 1993).

The difference of [CO_2] between substomatal cavities and chloroplasts is omitted, while diffusion related to dark-respiration and photorespiration are negligible and Eqn. (11) may be simplified to

$$\Delta_i = a + (b - a) \frac{C_i}{C_a}. \quad (12)$$

Eqn. (12) denotes the linear relationship between carbon discrimination and C_i/C_a. That underlines subsequent comparison between expected Δ (originating from gas-exchange, Δ_i, and measured Δ_{obs}), could evaluate the differences of [CO_2] between intercellular air and sites of carboxylation associated with ^{13}C fractionation from mesophyll conductance. Consequently, g_m is calculated by subtracting the Δ_{obs} of Eqn. (11) from Δ_i [Eqn. (12)]:

$$\Delta_i - \Delta_{obs} = (b - e_s - a_l) \frac{C_i - C_c}{C_a} + \frac{\frac{eR_D}{k} + f\Gamma^*}{C_a} \quad (13)$$

and P_n from Fick's first law is presented by

$$P_n = g_m(C_i - C_c). \quad (14)$$

Substituting Eqn. (14) into Eqn. (13) we obtain

$$\Delta_i - \Delta_{obs} = (b - e_s - a_l) \frac{P_n}{g_m C_a} + \frac{\frac{eR_D}{k} + f\Gamma^*}{C_a}, \text{ and} \quad (15)$$

$$g_m = \frac{(b - e_s - a_l)\frac{P_n}{C_a}}{(\Delta_i - \Delta_{obs}) - \frac{eR_D/k + f\Gamma^*}{C_a}}. \quad (16)$$

In the calculation of g_m, terms of respiratory and photorespiratory could be ignored and e and f are assumed to be zero or cancelled in the calculation of g_m.

Then Eqn. (16) can be rewritten as

$$g_m = \frac{(b-e_s-a_l)\frac{P_n}{C_a}}{\Delta_i-\Delta_{obs}}. \quad (17)$$

Therefore, the contribution of post- carboxylation fractionation can be estimated by

$$Contribution\ of\ post-\text{carboxylation}\ fractionation = \frac{(\text{Total } {}^{13}\text{C fractionation}-\text{fractionation from mesophll conductance})}{\text{Total } {}^{13}\text{C fractionation}} \times 100\%. \quad (18)$$

3 Results

3.1 Foliar gas exchange measurements

When SWC increased between the treatments, P_n, g_s and T_r in *P. orientalis* and *Q. variabilis* peaked at 70–80% of FC and/or 100% of FC (Fig. 2). The C_i in *P. orientalis* rose as SWC increased. It peaked at 60–70% of FC and declined thereafter with increased SWC in *Q. variabilis*. The carbon uptake and C_i were significantly improved by elevated [CO_2] at all SWC for the two species ($p< 0.05$). Greater increases of P_n in *P. orientalis* were found at 50–70% of FC from C_{400} to C_{800}, which was at 35–45% of FC in *Q. variabilis*. As water stress was reduced (at 70–80% and 100% of FC), reduction of g_s in *P. orientalis* was more pronounced with elevated [CO_2] at a given SWC ($p< 0.01$). Nevertheless, g_s in *Q. variabilis* for C_{400}, C_{500}, and C_{600} was significantly higher than that for C_{800} at 50–80% of FC ($p< 0.01$). Coordinated with g_s, T_r of the two species for C_{400} and C_{500} was significantly higher than that for C_{600} and C_{800}, except at 35–60% of FC ($p< 0.01$, Figs. 2g and 2h). P_n, g_s, C_i and T_r in *Q. variabilis* was significantly greater than the corresponding values in *P. orientalis* ($p< 0.01$, Fig. 2).

3.2 $\delta^{13}C$ of water-soluble compounds in leaves

After observations of photosynthetic traits in leaves of the two species, the same leaves were immediately frozen and WSCs were extracted for all orthogonal treatments. The carbon isotope composition of WSCs ($\delta^{13}C_{WSC}$) of both species increased as SWC increased (Figs. 3a and 3b, $p< 0.01$). The mean $\delta^{13}C_{WSC}$ of *P. orientalis* and *Q. variabilis* ranged from -27.44 ± 0.155‰ to -26.71 ± 0.133‰, and from -27.96 ± 0.129‰ to -26.49 ± 0.236‰, respectively. The photosynthetic capacity varied with increased SWC and the mean $\delta^{13}C_{WSC}$ of the two species, reaching their respective maxima at 70–80% of FC. With gradual enrichment of [CO_2], mean $\delta^{13}C_{WSC}$ in both species declined when [CO_2] exceeded 600 ppm ($p< 0.01$). Except for C_{400} at 50–100% of FC, the $\delta^{13}C_{WSC}$ in *P. orientalis* was significantly higher than that in *Q. variabilis* for most [CO_2] × SWC treatments ($p< 0.01$, Fig. 3).

3.3 Estimations of WUE_{ge} and WUE_{cp}

Figure 4a shows that increments of WUE_{ge} in *P. orientalis* under severe drought (i.e., 35–45% of FC) were highest for most [CO_2], ranging from 90.7% to 564.65%. The WUE_{ge} in *P. orientalis* decreased as SWC increased and increased as [CO_2] elevated. Differing from variation in WUE_{ge} in *P. orientalis* with moistened soil, WUE_{ge} in *Q. variabilis* increased slightly at 100% of FC for C_{600} or C_{800} (Fig. 4b). The maximum WUE_{ge} occurred at 35–45% of FC for C_{800} among all orthogonal treatments associated with both species. Elevated [CO_2] enhanced the WUE_{ge} in *Q. variabilis* at any SWC, except at 60–80% of FC. Thirty-two saplings of *P. orientalis* had greater WUE_{ge} than did *Q. variabilis* for the same [CO_2] × SWC treatments ($p< 0.05$).

As illustrated in Fig. 5a, WUE_{cp} in *P. orientalis* for C_{600} or C_{800} increased as water stress was alleviated beyond 50–60% of FC, as well as that for C_{400} or C_{500}, while SWC exceeded 60–70% of FC. *Q. variabilis* showed variable WUE_{cp} with increasing SWC (Fig. 5b). Except for C_{400}, WUE_{cp} in *Q. variabilis*

decreased abruptly at 50–60% of FC, and then increased as SWC increased for C_{500}, C_{600}, and C_{800}. In contrast to the results for WUE_{ge}, WUE_{cp} in *Q. variabilis* was more pronounced than in *P. orientalis* among all orthogonal treatments.

3.4 ^{13}C fractionation from the site of carboxylation to cytoplasm before sugar transportation

We evaluated the total ^{13}C fractionation from the site of carboxylation to the cytoplasm by gas-exchange measurements and WSCs in leaves (Table 2), which can help track the path of ^{13}C fractionation in leaves. Comparing $\delta^{13}C_{WSC}$ with $\delta^{13}C_{model}$ from Eqns. (4, 7–9), the total ^{13}C fractionation in *P. orientalis* ranged from 0.0328 to 0.0472‰, which was less than that in *Q. variabilis* (0.0384 to 0.0466‰). The total fractionation in *P. orientalis* was magnified with increasing SWC especially when SWC reached 35–80% of FC from C_{400} to C_{800} (increased by 21.30–42.04%). The total fractionation for C_{400} and C_{500} were amplified as SWC increased until 50–60% of FC in *Q. variabilis*, whereas they were increased at 50–80% of FC and decreased at 100% of FC for C_{600} and C_{800}. Elevated $[CO_2]$ enhanced the mean total fractionation in *P. orientalis*, while fractionation in *Q. variabilis* declined sharply from C_{600} to C_{800}. Total ^{13}C fractionation, with increased SWC, in *P. orientalis* increased more rapidly than it did in *Q. variabilis*.

3.5 g_m imposed on the interaction of CO_2 concentration and water stress

A comparison between online leaf $\delta^{13}C_{WSC}$ and the values of gas-exchange measurements is given to estimate the g_m over all treatments in Fig. 6 [Eqns. (10–17)]. A significant increasing trend occurred in g_m with decreasing water stress in *P. orientalis*, ranging from 0.0091–0.0690 mol·CO_2 $m^{-2}\cdot s^{-1}$ ($p< 0.05$), which reached a maximum at 100% of FC under a given $[CO_2]$. Increases in g_m in *Q. variabilis* with increasing SWC were not significant, except those under C_{400}. With increasing $[CO_2]$, g_m in the two species increased at different rates. With *P. orientalis* under C_{400}, g_m increased gradually and reached a maximum under C_{800} at 35–60% and 100% of FC ($p< 0.05$). However, that was maximized under C_{600} ($p< 0.05$) and reduced under C_{800} at 60–80% of FC. The maximum increment in g_m (8.2–58.4%) occurred at C_{800} at all SWC for *Q. variabilis*. The g_m in *Q. variabilis* was clearly greater than that in *P. orientalis* under the same treatments.

3.6 Contribution of post-carboxylation fractionation

We evaluated the difference between Δ_i and Δ_{obs} in ^{13}C fractionation derived from mesophyll conductance. The post-photosynthetic fractionation after carboxylation can be calculated by subtracting g_m-sourced fractionation from the total ^{13}C fractionation (Table 2). The g_m-sourced fractionation provided a smaller contribution to the total ^{13}C fractionation than did post-carboxylation fractionation irrespective of treatment (Table 2). The g_m-sourced fractionation in the two species illustrated different variations with increasing SWC, which declined at 50–80% of FC and increased at 100% of FC in *P. orientalis*; yet, in *Q. variabilis*, it increased with water stress alleviation at 50–80% of FC and then decreased at 100% of FC. Nevertheless, in the two species post-carboxylation fractionation in leaves all increased as SWC increased. The g_m-sourced fractionation in *P. orientalis* and *Q. variabilis* reached their peaks under C_{600} and C_{800}, respectively. Post-carboxylation fractionation was magnified with increases in $[CO_2]$ in *P. orientalis*, and reached a maximum under C_{600} and then declined under C_{800}.

3.7 Relationship between g_s, g_m and total ^{13}C fractionation

Total ^{13}C fractionation may be correlated with resistances associated with stomata and mesophyll cells. We performed linear regressions between g_s/g_m and total ^{13}C fractionation in *P. orientalis* and *Q. variabilis* (Fig. 7 and 8). The total ^{13}C fractionation was correlated to g_s ($p< 0.01$). The positive linear relationships between g_m and total ^{13}C fractionation ($p< 0.01$) indicated that the variation of $[CO_2]$

through the chloroplast was correlated with carbon discrimination following leaf photosynthesis.

4 Discussion

4.1 Photosynthetic traits

The exchange of CO_2 and water vapor via stomata can be modulated by the soil/leaf water potential (Robredo et al., 2010). Saplings of *P. orientalis* reached maximum P_n and g_s at 70–80% of FC irrespective of [CO_2] treatments. As SWC exceeded this soil water threshold, elevated CO_2 caused a greater reduction in g_s as was previously reported for barley and wheat (Wall et al., 2011). The decrease in g_s responding to elevated [CO_2], could be mitigated with ~~increased~~ increases in SWC. The C_i in *Q. variabilis* peaked at 60–70% of FC and then declined as soil moisture increased (Wall et al., 2006; Wall et al., 2011). This may be because stomata tend to maintain a constant C_i or C_i/C_a when ambient [CO_2] is increased, which would determine the amount of CO_2 used directly in the chloroplast (Yu et al., 2010). This result could be explained as stomatal limitation (Farquhar and Sharkey, 1982; Xu, 1997). However, C_i in *P. orientalis* increased considerably, while SWC exceeded 70–80% of FC, as found by Mielke et al. (2000). One possible contributing factor is plants close their stomata to reduce water loss during organic matter synthesis simultaneously decreasing the availability of CO_2 and generating respiration of organic matter (Robredo et al., 2007). Another possible explanation is that the limited root volume of potted plants may be unable to absorb sufficient water to support the full growth of shoots (Leakey et al., 2009; Wall et al., 2011). In the present study, increasing [CO_2] may cause nonstomatal limitation when SWC exceeds a soil moisture threshold of 70–80% of FC. The accumulation of nonstructural carbohydrates in leaf tissue may induce mesophyll-based and/or biochemical-based transient inhibition of photosynthetic capacity (Farquhar and Sharkey, 1982). Xu and Zhou (2011) developed a five-level SWC gradient to examine the effect of water on the physiology of a perennial, *Leymus chinensis*, and demonstrated that there was a clear maximum in SWC, below which the plant could adjust to changing environmental conditions. Micanda-Apodaca et al. (2014) also concluded that in suitable water conditions, elevated CO_2 levels augmented CO_2 assimilation in herbaceous plants.

The P_n of the two woody plant species increased with elevated [CO_2] similar to results seen with other C_3 woody plants (Kgope et al., 2010). Increasing [CO_2] alleviated severe drought and the need for heavy irrigation, suggesting that photosynthetic inhibition produced by a lack or excess of water may be mediated by increased [CO_2] (Robredo et al., 2007; Robredo et al., 2010) and ameliorate the effects of drought stress by reducing plant transpiration (Kirkham, 2016; Kadam et al., 2014; Micanda-Apodaca et al., 2014; Tausz-Posch et al., 2013).

4.2 Differences between WUE_{ge} and WUE_{cp}

Increases in WUE_{ge} in *P. orientalis* and *Q. variabilis* that resulted from the combination of P_n increase and g_s decrease were followed by a reduction in T_r (Figs. 2a, 2g, 2b and 2h). This result was also demonstrated by Ainsworth and McGrath (2010). Comparing P_n and T_r in the two species, a lower WUE_{ge} in *Q. variabilis* was obtained due to its different physiological and morphological traits, such as larger leaf area, rapid growth, and higher stomatal conductance than that in *P. orientalis* (Adiredjo et al., 2014). Medlyn et al. (2001) reported that stomatal conductance of broadleaved species is more sensitive to elevated [CO_2] than conifer species. There is no agreement on the patterns of iWUE at the leaf level, related to SWC (Yang et al., 2010). The WUE_{ge} in *P. orientalis* and *Q. variabilis* were enhanced with soil drying, as presented by Parker and Pallardy (1991), DeLucia and Heckathorn (1989), Reich et al. (1989), and Leakey (2009).

Bögelein et al. (2012) confirmed that WUE_{cp} was more consistent with daily mean WUE_{ge} than with WUE_{phloem} (calculated with the $\delta^{13}C$ of phloem). The WUE_{cp} of the two species demonstrated similar variations to those in $\delta^{13}C_{WSC}$, which differed from those of WUE_{ge}. Pons et al. (2009) noted that Δ of leaf soluble sugar is coupled with environmental dynamics over a period ranging from a few hours to 1–2 days. The WUE_{cp} of our materials responded to $[CO_2]$ × SWC treatments over a number of ~~cultivated~~ days, whereas WUE_{ge} was characterized as the instantaneous physiological change in plants to new conditions. Consequently, WUE_{cp} and WUE_{ge} had different degrees of variations in response to different treatments.

4.3 Influence of mesophyll conductance on the fractionation after carboxylation

Mesophyll conductance, g_m, has been identified to coordinate with environmental factors more rapidly than stomatal conductance (Galmés et al., 2007; Tazoe et al., 2011; Flexas et al., 2007). During our 7-day cultivations, g_m increased and WUE_{ge} decreased with increasing SWC. It has been documented that g_m can improve WUE under drought pretreatment (Han et al., 2016). However, the mechanism by which g_m responds to the fluctuation of $[CO_2]$ is unclear. Terashima *et al.* (2006) demonstrated that CO_2 permeable aquaporin, located in the plasma membrane and inner envelope of chloroplasts, could regulate the change in g_m. In our study, g_m is species-specific to the $[CO_2]$ gradient. The g_m in *P. orientalis* significantly decreased by 9.0%-44.4% from C_{600} to C_{800} at 60-80% of FC; these are similar to the results of Flexas *et al.* (2007). A larger g_m in *Q. variabilis* under C_{800} was observed compared to *P. orientalis*.

Furthermore, g_m contributed to the total ^{13}C fractionation that followed carboxylation, while photosynthate had not been transported to the sapling twigs. The ^{13}C fractionation of CO_2 from the air surrounding the leaf to sub-stomatal cavities may be simply explained by stomatal resistance, which also contains the fractionation derived from mesophyll conductance between sub-stomatic cavities and the site of carboxylation in the chloroplast that cannot be neglected and should be elucidated (Pons et al., 2009; Cano et al., 2014). In estimating the post-carboxylation fractionation, g_m-sourced fractionation must be subtracted from the total ^{13}C fractionation (the difference between $\delta^{13}C_{WSC}$ and $\delta^{13}C_{model}$), which is closely associated with g_m (Fig. 8, p= 0.01). Variations in g_m-sourced fractionation are coordinated with those in g_m with changing environmental conditions (Table 2).

4.4 Post-carboxylation fractionation generated before photosynthate moves out of leaves

Photosynthesis, a biochemical and physiological process (Badeck et al., 2005), is characterized by discrimination in ^{13}C, which leaves an isotopic signature in the photosynthetic apparatus. Farquhar *et al.* (1989) reviewed the carbon-fractionation in leaves and covered the significant aspects of photosynthetic carbon isotope discrimination. The post-carboxylation/photosynthetic fractionation associated with the metabolic pathways of non-structural carbohydrates (NSC; defined here as soluble sugars + starch) within leaves, and fractionation during translocation, storage, and remobilization prior to tree ring formation is unclear (Epron et al., 2012; Gessler et al., 2014; Rinne et al., 2016). The synthesis of sucrose and starch before transportation to twigs falls within the domain of post-carboxylation fractionation generated in leaves. Hence, we hypothesized that ^{13}C fractionation ~~might~~ may exist. When we completed the leaf gas-exchange measurements, leaf samples were collected immediately to determine the $\delta^{13}C_{WSC}$. Presumably, ^{13}C fractionation generated in the synthetic processes of sucrose and starch was contained within the ^{13}C fractionation from the site of carboxylation to cytoplasm before sugar transportation. Comparing $\delta^{13}C_{WSC}$ with $\delta^{13}C_{obs}$, the total ^{13}C fractionation in *P. orientalis* ranged from 0.0328 to 0.0472‰, which was somewhat less than that in *Q. variabilis* (from 0.0384 to 0.0466‰). Post-carboxylation fractionation contributed 75.30-98.9% to total ^{13}C fractionation, determined by subtracting

the fractionation in g_m from total ^{13}C fractionation. Gessler et al. (2004) reviewed the environmental components of variation in photosynthetic carbon isotope discrimination in terrestrial plants. Total ^{13}C fractionation in *P. orientalis* was enhanced by the increase in SWC, consistent with that in *Q. variabilis*, except at 100% of FC. The ^{13}C isotope signature in *P. orientalis* was depleted with elevated $[CO_2]$. Yet, ^{13}C-depletion was weakened in *Q. variabilis* for C_{600} and C_{800}. Linear regressions between g_s and total ^{13}C fractionation indicated that the post-carboxylation fractionation in leaves depends on the variation of g_s and that stomata aperture was correlated with environmental change.

5 Conclusions

Through orthogonal treatments of four $[CO_2]$ × five SWC, WUE_{cp} calculated by $\delta^{13}C_{WSC}$ and WUE_{ge} derived from simultaneous leaf gas-exchange, were estimated to differentiate the $\delta^{13}C$ signal variation before leaf-level translocation of primary assimilates. The influence of g_m on ^{13}C fractionation between the sites of carboxylation and ambient air is important. It requires consideration when testing the hypothesis that the post-carboxylation contributes to the ^{13}C fractionation from the site of carboxylation to cytoplasm before sugar transport. In response to the interactive effects of $[CO_2]$ and SWC, WUE_{ge} in the two tree species both decreased with increasing SWC, and increased with elevated $[CO_2]$ at 35–80% of FC. We concluded that relative soil drying, coupled with elevated $[CO_2]$, can improve WUE_{ge} by strengthening photosynthetic capacity and reducing transpiration. WUE_{ge} in *P. orientalis* was significantly greater than that in *Q. variabilis*, while the opposite was the case for WUE_{cp}. The g_m and post-carboxylation both contributed to the total ^{13}C fractionation. Rising $[CO_2]$ and/or moistening soil generated increasing disparities between $\delta^{13}C_{WSC}$ and $\delta^{13}C_{model}$ in *P. orientalis*; nevertheless, the differences between $\delta^{13}C_{WSC}$ and $\delta^{13}C_{model}$ in *Q. variabilis* increased when $[CO_2]$ was less than 600 ppm and/or water stress was alleviated. Total ^{13}C fractionation in the leaf was linearly dependent on g_s. With respect to carbon isotope fractionation in post-carboxylation and transportation processes, we note that ^{13}C fractionation derived from the synthesis of sucrose and starch is likely influenced by environmental changes. A clear description of the magnitude and environmental dependence of post-carboxylation fractionation is worth considering.

References

Adiredjo, A. L., Navaud, O., Lamaze, T., and Grieu, P.: Leaf carbon isotope discrimination as an accurate indicator of water use efficiency in sunflower genotypes subjected to five stable soil water contents, J Agron. Crop Sci., 200, 416–424, 2014.

Ainsworth, E. A. and McGrath, J. M.: Direct effects of rising atmospheric carbon dioxide and ozone on crop yields, Climate Change and Food Security, Springer, 109–130, 2010.

Badeck, F. W., Tcherkez, G., Eacute, N. S. S., Piel, C. E. M., and Ghashghaie, J.: Post-photosynthetic fractionation of stable carbon isotopes between plant organ – a widespread phenomenon, Rapid Commun. Mass S., 19, 1381–1391, 2005.

Bögelein, R., Hassdenteufel, M., Thomas, F. M., and Werner, W.: Comparison of leaf gas exchange and stable isotope signature of water-soluble compounds along canopy gradients of co-occurring Douglas-fir and European beech, Plant Cell Environ., 35, 1245–1257, 2012.

Brandes, E., Kodama, N., Whittaker, K., Weston, C., Rennenberg, H., Keitel, C., Adams, M. A., and Gessler, A.: Short-term variation in the isotopic composition of organic matter allocated from the leaves to the stem of *Pinus sylvestris*: effects of photosynthetic and postphotosynthetic carbon

439 isotope fractionation, Global Change Biol., 12, 1922–1939, 2006.
440 Brooks, A. and Farquhar, G. D.: Effect of temperature on the CO_2/O_2 specificity of ribulose-1,5-
441 bisphosphate carboxylase/oxygenase and the rate of respiration in the light, Planta, 165, 397–406,
442 1985.
443 Brugnoli E, Farquhar GD. 2000. Photosynthetic fractionation of carbon isotopes. In: Leegood RC,
444 Sharkey TD, von Caemmerer S. eds. Photosynthesis: physiology and metabolism. Advances in
445 photosynthesis. Dordrecht, The Netherlands: Kluwer Academic Publishers, 399–434.
446 Cano, F. J., López, R., and Warren, C. R.: Implications of the mesophyll conductance to CO_2 for
447 photosynthesis and water-use efficiency during long-term water stress and recovery in two
448 contrasting Eucalyptus species, Plant Cell Environ., 37, 2470–2490, 2014.
449 Cernusak, L. A., Ubierna, N., Winter, K., Holtum, J. A. M., Marshall, J. D., and Farquhar, G. D.:
450 Environmental and physiological determinants of carbon isotope discrimination in terrestrial plants,
451 New Phytologist, 200, 950–965, 2013.
452 DeLucia, E. H. and Heckathorn, S. A.: The effect of soil drought on water-use efficiency in a contrasting
453 Great Basin desert and Sierran montane species, Plant Cell Environ., 12, 935–940, 1989.
454 Epron, D., Nouvellon, Y., and Ryan, M. G.: Introduction to the invited issue on carbon allocation of trees
455 and forests, Tree physiol., 32, 639–643, 2012.
456 Evans, J. R., Kaldenhoff, R., Genty, B., and Terashima, I.: Resistances along the CO_2 diffusion pathway
457 inside leaves, J. Exp. Bot., 60, 2235–2248, 2009.
458 Evans, J. R., Sharkey, T. D., Berry, J. A., and Farquhar, G. D.: Carbon isotope discrimination measured
459 concurrently with gas-exchange to investigate CO_2 diffusion in leaves of higher-plants, Funct. Plant
460 Biol., 13, 281–292, 1986.
461 Evans, J. R. and von Caemmerer, S.: Temperature response of carbon isotope discrimination and
462 mesophyll conductance in tobacco, Plant Cell Environ., 36, 745–756, 2013.
463 Farquhar, G. D., Ehleringer, J. R., and Hubick, K. T.: Carbon isotope discrimination and photosynthesis,
464 Ann. Rev. Plant Physiol., 40, 503–537, 1989.
465 Farquhar, G. D., O'Leary, M. H., and Berry, J. A.: On the relationship between carbon isotope
466 discrimination and the intercellular carbon dioxide concentration in leaves, Funct. Plant Biol., 9,
467 121–137, 1982.
468 Farquhar, G. D. and Sharkey, T. D.: Stomatal conductance and photosynthesis, Ann. Rev. Plant Physiol.,
469 33, 317–345, 1982.
470 Flexas, J., Barbour, M. M., Brendel, O., Cabrera, H. M., Carriquí, M., Díaz-Espejo, A., Douthe, C.,
471 Dreyer, E., Ferrio, J. P., Gago, J., Gallé, A., Galmés, J., Kodama, N., Medrano, H., Niinemets, Ü.,
472 Peguero-Pina, J. J., Pou, A., Ribas-Carbó, M., Tomás, M., Tosens, T., and Warren, C. R.: Mesophyll
473 diffusion conductance to CO_2: An unappreciated central player in photosynthesis, Plant Science,
474 193–194, 70–84, 2012.
475 Flexas, J., Carriquí, M., Coopman, R. E., Gago, J., Galmés, J., Martorell, S., Morales, F., and Diaz-
476 Espejo, A.: Stomatal and mesophyll conductances to CO_2 in different plant groups: Underrated
477 factors for predicting leaf photosynthesis responses to climate change? Plant Science, 226, 41–48,
478 2014.
479 Flexas, J., Diaz-Espejo, A., Galmés, J., Kaldenhoff, R., Medano, H., and Ribas-Carbo, M.: Rapid
480 variations of mesophyll conductance in response to changes in CO_2 concentration around leaves,
481 Plant Cell Environ., 30, 1284–1298, 2007.
482 Flexas, J., Ribas-Carbó, M., Diaz-Espejo, A., Galmés, J., and Medrano, H.: Mesophyll conductance to

CO_2: current knowledge and future prospects, Plant Cell Environ., 31, 602–621, 2008.

Flexas, J., Ribas-Carbó, M., Hanson, D.T., Bota, J., Otto, B., Cifre, J., McDowell, N., Medrano, H., and Kaldenhoff, R.: Tobacco aquaporin NtAQP1 is involved in mesophyll conductance to CO_2 *in vivo*, Plant J., 48, 427–439, 2006.

Galmés, J., Medrano, H., and Flexas, J.: Photosynthetic limitations in response to water stress and recovery in Mediterranean plants with different growth forms, New Phytol., 175, 81–93. 2007.

Gessler, A., Brandes, E., Buchmann, N., Helle, G., Rennenberg, H., and Barnard, R. L.: Tracing carbon and oxygen isotope signals from newly assimilated sugars in the leaves to the tree-ring archive, Plant Cell Environ., 32, 780–795, 2009.

Gessler, A., Ferrio, J. P., Hommel, R., Treydte, K., Werner, R. A., and Monson, R. K.: Stable isotopes in tree rings: towards a mechanistic understanding of isotope fractionation and mixing processes from the leaves to the wood, Tree Physiol., 34, 796–818, 2014.

Gessler, A., Rennenberg, H., and Keitel, C.: Stable isotope composition of organic compounds transported in the phloem of European beech-evaluation of different methods of phloem sap collection and assessment of gradients in carbon isotope composition during leaf-to-stem transport, Plant Biology, 6, 721–729, 2004.

Gessler, A., Tcherkez, G., Peuke, A. D., Ghashghaie, J., and Farquhar, G. D.: Experimental evidence for diel variations of the carbon isotope composition in leaf, stem and phloem sap organic matter in *Ricinus communis*, Plant Cell Environ., 31, 941–953, 2008.

Gillon, J. S., Griffiths, H.: The influence of (photo)respiration on carbon isotope discrimination in plants. Plant Cell Environ., 20, 1217–1230, 1997.

Gleixner, G. and Schmidt, H.: Carbon isotope effects on the fructose-1, 6-bisphosphate aldolase reaction, origin for non-statistical ^{13}C distributions in carbohydrates, J. Biol. Chem., 272, 5382–5387, 1997.

Guy, R. D., Fogel, M. L., and Berry, J. A.: Photosynthetic fractionation of the stable isotopes of oxygen and carbon, Plant Physiol., 101, 37–47, 1993.

Han, J. M., Meng, H. F., Wang, S. Y., Jiang, C. D., Liu, F., Zhang, W. F., and Zhang, Y. L.: Variability of mesophyll conductance and its relationship with water use efficiency in cotton leaves under drought pretreatment, J. Plant Physiol., 194, 61–71, 2016.

Hommel, R., Siegwolf, R., Saurer, M., Farquhar, G. D., Kayler, Z., Ferrio, J. P., and Gessler, A.: Drought response of mesophyll conductance in forest understory species-impacts on water-use efficiency and interactions with leaf water movement, Physiol. Plantarum, 152, 98–114, 2014.

Igamberdiev, A. U., Mikkelsen, T. N., Ambus, P., Bauwe, H., and Lea, P. J.: Photorespiration contributes to stomatal regulation and carbon isotope fractionation: a study with barley, potato and Arabidopsis plants deficient in glycine decarboxylase, Photosynth. Res., 81, 139–152, 2004.

IPCC: Summary for policymakers, in: Climate Change 2014, Mitigation of Climate Change, contribution of Working Group III to the Fifth Assessment Report of the Intergovernmental Panel on Climate Change, edited by: Edenhofer, O., Pichs-Madruga, R., Sokona, Y., Farahani, E., Kadner, S., Seyboth, K., Adler, A., Baum, I., Brunner, S., Eickemeier, P., Kriemann, B., Savolainen, J., Schlomer, S., von Stechow, C., Zwickel, T., and Minx, J. C., Cambridge University Press, Cambridge, UK and New York, NY, USA, 1–30, 2014.

Jäggi, M., Saurer, M., Fuhrer, J., and Siegwolf, R.: The relationship between the stable carbon isotope composition of needle bulk material, starch, and tree rings in *Picea abies*, Oecologia, 131, 325–332, 2002.

Kadam, N. N., Xiao, G., Melgar, R. J., Bahuguna, R. N., Quinones, C., Tamilselvan, A., Prasad, P. V.

V., and Jagadish, K. S. V.: Chapter three-agronomic and physiological responses to high temperature, drought, and elevated CO_2 interactions in cereals, Adv. Agron., 127, 111–156, 2014.

Kgope, B. S., Bond, W. J., and Midgley, G. F.: Growth responses of African savanna trees implicate atmospheric [CO_2] as a driver of past and current changes in savanna tree cover, Austral Ecol., 35, 451–463, 2010.

Kirkham, M. B.: Elevated carbon dioxide: impacts on soil and plant water relations, CRC Press, London, New York, 2016.

Kodama, N., Barnard, R. L., Salmon, Y., Weston, C., Ferrio, J. P., Holst, J., Werner, R. A., Saurer, M., Rennenberg, H., and Buchmann, N.: Temporal dynamics of the carbon isotope composition in a *Pinus sylvestris* stand: from newly assimilated organic carbon to respired carbon dioxide, Oecologia, 156, 737–750, 2008.

Lanigan, G. J., Betson, N., Griffiths, H., and Seibt, U.: Carbon isotope fractionation during photorespiration and carboxylation in Senecio, Plant Physiol., 148, 2013–2020, 2008.

Le Roux, X., Bariac, T., Sinoquet H., Genty, B., Piel, C., Mariotti, A., Girardin, C., and Richard, P.: Spatial distribution of leaf water-use efficiency and carbon isotope discrimination within an isolated tree crown, Plant Cell Environ., 24, 1021–1032, 2001.

Leakey, A. D.: Rising atmospheric carbon dioxide concentration and the future of C4 crops for food and fuel, Proceedings of the Royal Society of London B: Biological Sciences, 276, 1517–2008, 2009.

Leakey, A. D., Ainsworth, E. A., Bernacchi, C. J., Rogers, A., Long, S. P., and Ort, D. R.: Elevated CO_2 effects on plant carbon, nitrogen, and water relations: six important lessons from FACE, J. Exp. Bot., 60, 2859–2876, 2009.

Lobell, D. B., Roberts, M. J., Schlenker, W., Braun, N., Little, B. B., Rejesus, R. M., and Hammer, G. L.: Greater sensitivity to drought accompanies maize yield increase in the US Midwest, Science, 344, 516–519, 2014.

Medlyn, B. E., Barton, C. V. M., Broadmeadow, M. S. J., Ceulemans, R., Angelis, P. D., Forstreuter, M., Freeman, M., Jackson, S. B., Kellomäki, S., and Laitat, E.: Stomatal conductance of forest species after long-term exposure to elevated CO_2 concentration: a synthesis, New Phytol., 149, 247–264, 2001.

Mielke, M. S., Oliva, M. A., de Barros, N. F., Penchel, R. M., Martinez, C. A., Da Fonseca, S., and de Almeida, A. C.: Leaf gas exchange in a clonal eucalypt plantation as related to soil moisture, leaf water potential and microclimate variables, Trees, 14, 263–270, 2000.

Micanda Apodaca, J., Pérez López, U., Lacuesta, M., Mena Petite, A., and Muñoz Rueda, A.: The type of competition modulates the ecophysiological response of grassland species to elevated CO_2 and drought, Plant Biolog, 17, 298–310, 2014.

Parker, W. C. and Pallardy, S. G.: Gas exchange during a soil drying cycle in seedlings of four black walnut (*Juglans nigra* l.) Families, Tree physiol., 9, 339–348, 1991.

Pons, T. L., Flexas, J., von Caemmerer, S., Evans, J. R., Genty, B., Ribas-Carbo, M., and Brugnoli, E.: Estimating mesophyll conductance to CO_2: methodology, potential errors, and recommendations, J. Exp. Bot., 8, 1–18, 2009.

Reich, P. B., Walters, M. B., and Tabone, T. J.: Response of *Ulmus americana* seedlings to varying nitrogen and water status. 2 Water and nitrogen use efficiency in photosynthesis, Tree Physiol., 5, 173–184, 1989.

Rinne, K. T., Saurer, M., Kirdyanov, A. V., Bryukhanova, M. V., Prokushkin, A. S., Churakova Sidorova, O. V., and Siegwolf, R. T.: Examining the response of larch needle carbohydrates to climate using

571 compound-specific $\delta^{13}C$ and concentration analyses, EGU General Assembly Conference,
572 1814949R, 2016.
573 Robredo, A., Pérez-López, U., de la Maza, H. S., González-Moro, B., Lacuesta, M., Mena-Petit,e A., and
574 Muñoz-Rueda, A.: Elevated CO_2 alleviates the impact of drought on barley improving water status
575 by lowering stomatal conductance and delaying its effects on photosynthesis, Environ. Exp. Bot.,
576 59, 252–263, 2007.
577 Robredo, A., Pérez-López, U., Lacuesta, M., Mena-Petite, A., and Muñoz-Rueda, A.: Influence of water
578 stress on photosynthetic characteristics in barley plants under ambient and elevated CO_2
579 concentrations, Biologia. Plantarum, 54, 285–292, 2010.
580 Rossmann, A., Butzenlechner, M., and Schmidt, H.: Evidence for a nonstatistical carbon isotope
581 distribution in natural glucose, Plant Physiol., 96, 609–614, 1991.
582 Streit, K., Rinne, K. T., Hagedorn, F., Dawes, M. A., Saurer, M., Hoch, G., Werner, R. A., Buchmann,
583 N., and Siegwolf, R. T. W.: Tracing fresh assimilates through *Larix decidua* exposed to elevated
584 CO_2 and soil warming at the alpine treeline using compound-specific stable isotope analysis, New
585 Phytol., 197, 838–849, 2013.
586 Tausz Posch, S., Norton, R. M., Seneweera, S., Fitzgerald, G. J., and Tausz, M.: Will intra-specific
587 differences in transpiration efficiency in wheat be maintained in a high CO_2 world? A FACE study,
588 Physiol. Plantarum, 148, 232–245, 2013.
589 Tazoe, Y., von Caemmerer, S., Estavillo, G. M., and Evans, J. R.: Using tunable diode laser spectroscopy
590 to measure carbon isotope discrimination and mesophyll conductance to CO_2 diffusion dynamically
591 at different CO_2 concentrations, Plant Cell Environ., 34, 580–591, 2011.
592 Terashima, I., Hanba, Y.T., Tazoe, Y., Vyas, P., and Yano, S.: Irradiance and phenotype: comparative
593 eco-development of sun and shade leaves in relation to photosynthetic CO_2 diffusion, J. Exp. Bot.,
594 57, 343–354, 2006.
595 Théroux-Rancourt, G., Éthier, G., and Pepin, S.: Threshold response of mesophyll CO_2 conductance to
596 leaf hydraulics in highly transpiring hybrid poplar clones exposed to soil drying, J. Exp. Bot., 65,
597 741-753, 2014.
598 Von Caemmerer, S. V. and Farquhar, G. D.: Some relationships between the biochemistry of
599 photosynthesis and the gas exchange of leaves, Planta, 153, 376–387, 1981.
600 Wall, G. W., Garcia, R. L., Kimball, B. A., Hunsaker, D. J., Pinter, P. J., Long, S. P., Osborne, C. P.,
601 Hendrix, D. L., Wechsung, F., and Wechsung, G.: Interactive effects of elevated carbon dioxide and
602 drought on wheat, Agron. J., 98, 354–381, 2006.
603 Wall, G. W., Garcia, R. L., Wechsung, F., and Kimball, B. A.: Elevated atmospheric CO_2 and drought
604 effects on leaf gas exchange properties of barley, Agr. Ecosyst. Environ., 144, 390–404, 2011.
605 Warren, C. R. and Adams, M. A.: Internal conductance does not scale with photosynthetic capacity:
606 implications for carbon isotope discrimination and the economics of water and nitrogen use in
607 photosynthesis, Plant Cell Environ., 29, 192–201, 2006.
608 Xu, D. Q.: Some problems in stomatal limitation analysis of photosynthesis, Plant Physiol. J., 33, 241–
609 244, 1997.
610 Xu, Z. and Zhou, G.: Responses of photosynthetic capacity to soil moisture gradient in perennial rhizome
611 grass and perennial bunchgrass, BMC Plant Boil., 11, 21, 2011.
612 Yang, B., Pallardy, S. G., Meyers, T. P., GU, L. H., Hanson, P. J., Wullschleger, S. D., Heuer, M.,
613 Hosman, K. P., Riggs, J. S., and Sluss D. W.: Environmental controls on water use efficiency during
614 severe drought in an Ozark Forest in Missouri, USA, Global Change Biol., 16, 2252–2271, 2010.

615 Yu, G., Wang, Q., and Mi, N.: Ecophysiology of plant photosynthesis, transpiration, and water use,
616 Science Press, Beijing, China, 2010.
617

618 **Author contributions**

619 N. Zhao and Y. He collected field samples, and performed the experiments. N. Zhao analyzed the data
620 and wrote the paper. P. Meng commented on the theory and study design. X. Yu revised and edited the
621 manuscript.
622

623 *Acknowledgements.* Financial support for this project was provided by the National Natural Science
624 Foundation of China (grant No. 41430747) and the Beijing Municipal Education Commission (CEFF-
625 PXM2017_014207_000043). We thank Beibei Zhou and Yuanhai Lou for collection of materials and
626 management of saplings. We are grateful to anonymous reviewers for constructive suggestions regarding
627 this manuscript. Due to space limitations we cited selected references involving this study topic and
628 apologize for authors whose work was not cited.

629

Figure

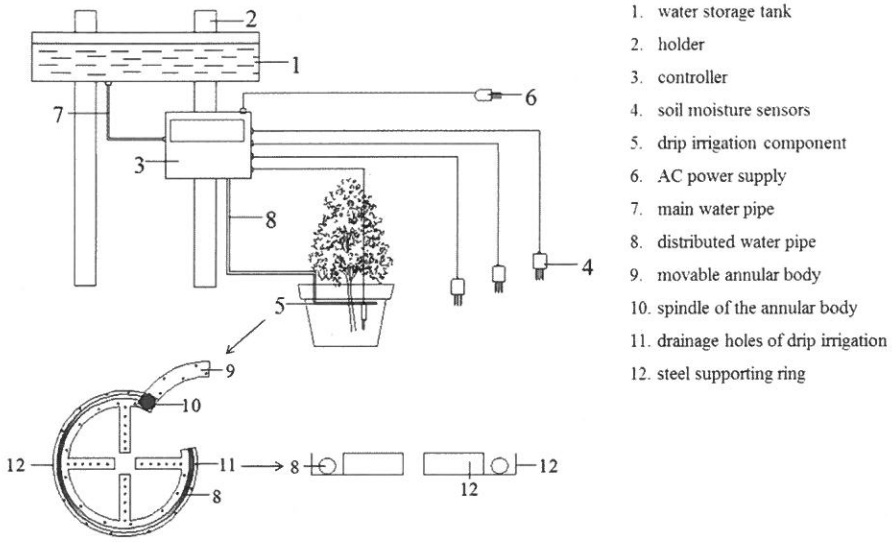

630 **Figure 1.** Diagram of the automatic drip irrigation device used in this study; numbers indicate the
631 individual parts of the irrigation device (No. 1–12). The lower-left corner of this figure presents the
632 detailed schematic for the drip irrigation component (No. 8–12).

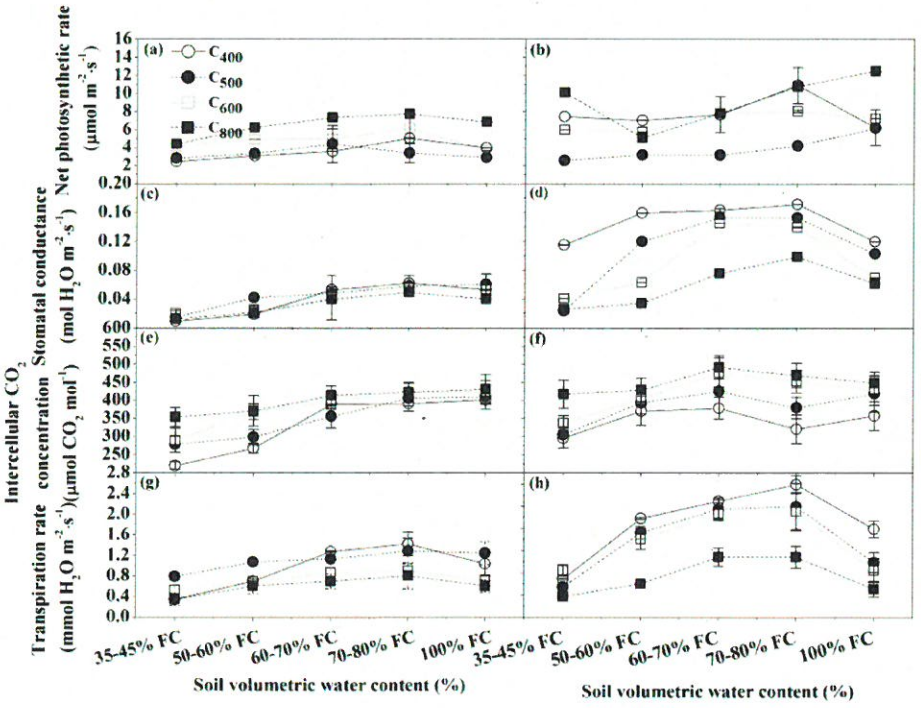

633 **Figure 2.** Net photosynthetic rates (P_n, μmol m^{-2} s^{-1}, a and b), stomatal conductance (g_s, mol H_2O m^{-2} s^{-1}, c and d), intercellular CO_2 concentration (C_i, μmol CO_2 mol^{-1}, e and f), and transpiration rates (T_r, mmol H_2O m^{-2} s^{-1}, g and h) in *P. orientalis* and *Q. variabilis* for four CO_2 concentration × five soil volumetric water content treatments. Means ± SDs, n= 32.

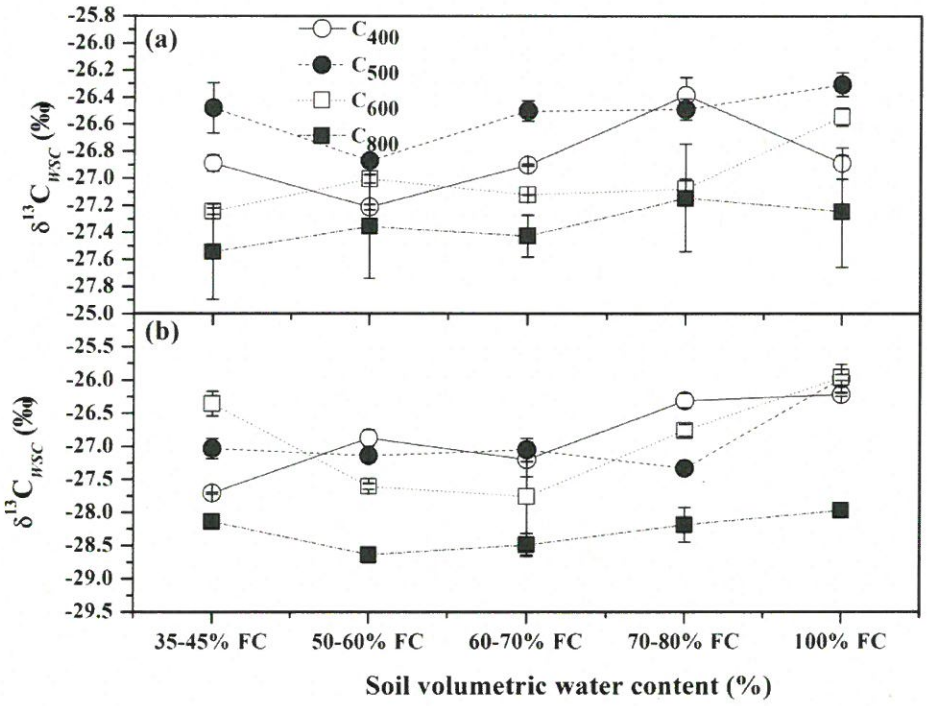

637 **Figure 3.** Carbon isotope composition of water-soluble compounds ($\delta^{13}C_{WSC}$) extracted from leaves of *P.*
638 *orientalis* (a) and *Q. variabilis* (b) for four CO_2 concentration × five soil volumetric water content
639 treatments. Means ± SDs, n= 32.

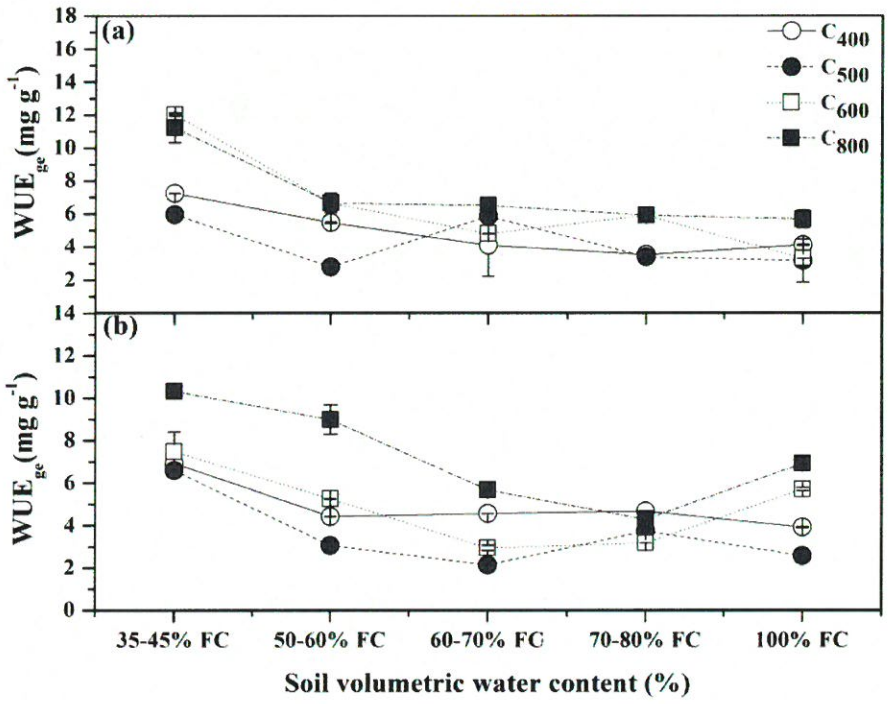

Figure 4. Instantaneous water use efficiency through gas exchange measurements (WUE_{ge}) for leaves from *P. orientalis* (a) and *Q. variabilis* (b) for four CO_2 concentration × five soil volumetric water content treatments. Means ± SDs, n= 32.

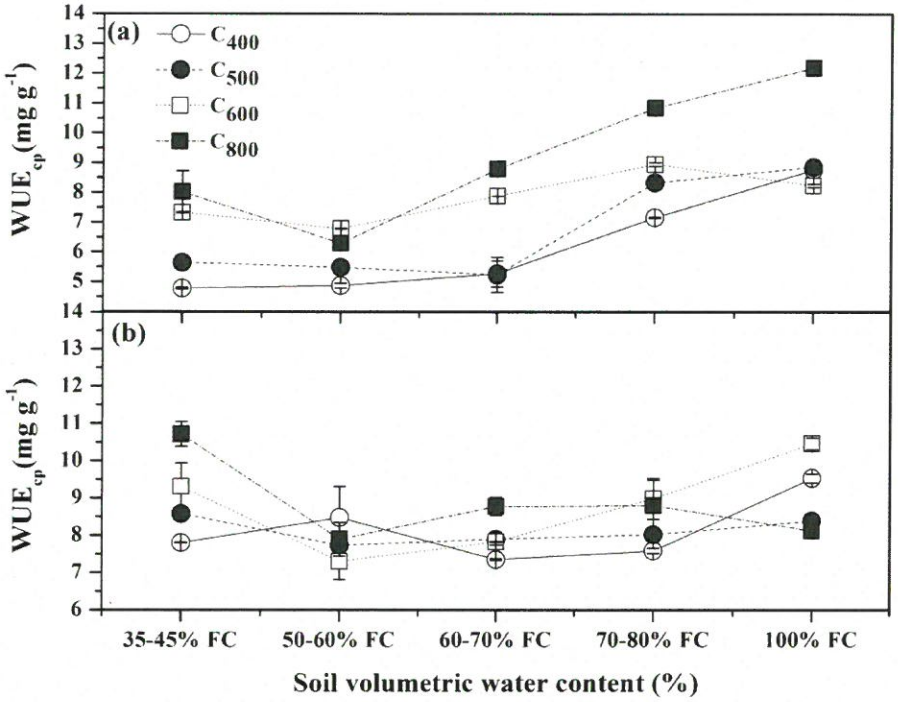

643 **Figure 5.** Instantaneous water use efficiency estimated by $\delta^{13}C$ of water-soluble compounds (WUE_{cp})
644 from leaves of *P. orientalis* (a) and *Q. variabilis* (b) for four CO_2 concentration × five soil volumetric
645 water content treatments. Means ± SDs, n= 32.

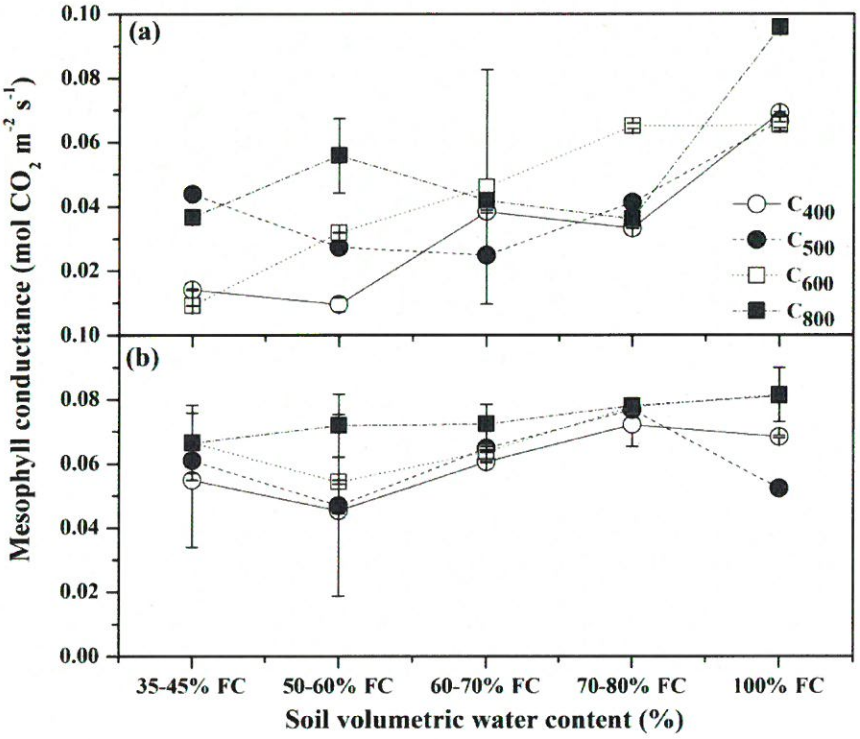

646 **Figure 6.** Mesophyll conductance in *P. orientalis* (a) and *Q. variabilis* (b) for four CO_2 concentration ×
647 five soil volumetric water content treatments. Means ± SDs, n= 32.

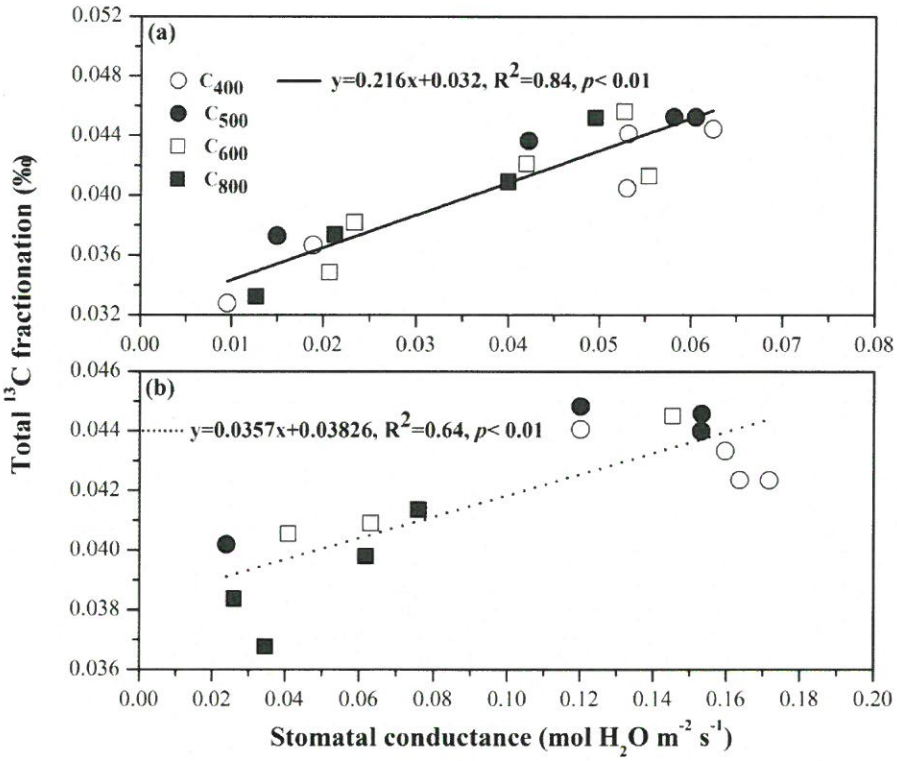

Figure 7. Regressions between stomatal conductance and total ^{13}C fractionation in *P. orientalis* (a) and *Q. variabilis* (b) for four CO_2 concentration × five soil volumetric water content treatments ($p< 0.01$, n= 32).

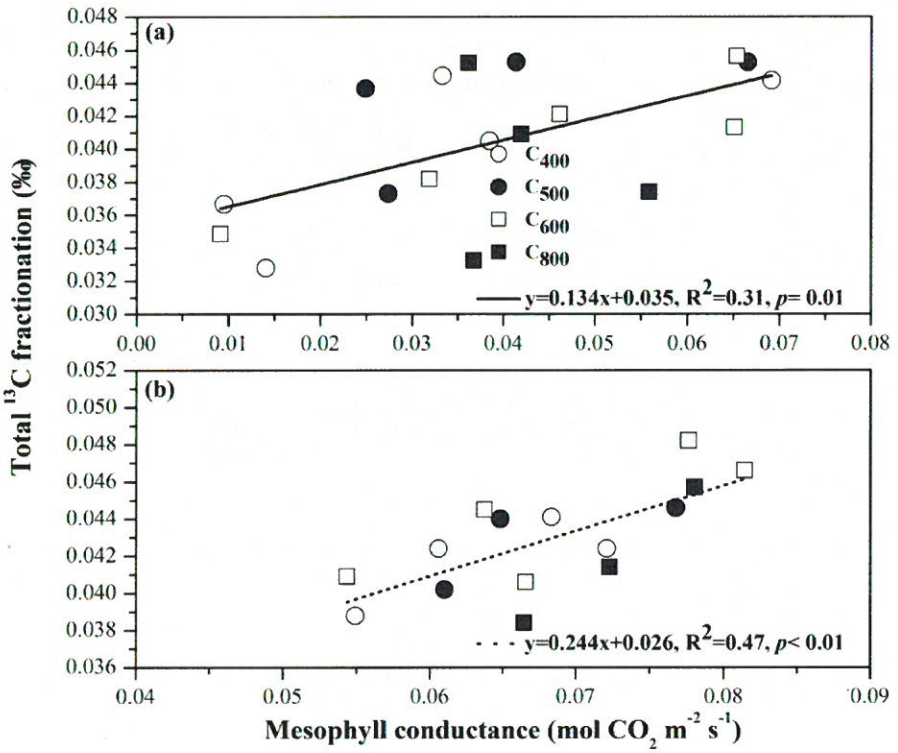

651 **Figure 8.** Regressions between mesophyll conductance and total ^{13}C fractionation in *P. orientalis* (a)
652 and *Q. variabilis* (b) for four CO_2 concentration × five soil volumetric water content treatments ($p \leq$
653 0.01, n= 32).

Table 2. Carbon-13 isotope fractionation in *P. orientalis* and *Q. variabilis* under four CO_2 concentration × five soil volumetric water content treatments.

Species	SWC (of FC)		CO_2 concentration (ppm)													
			400	500	600	800	^{13}C fractionation (‰)	400	500	600	800	^{13}C fractionation (‰)	400	500	600	800
P. orientalis	35–45%	Total ^{13}C fractionation (‰)	0.0328	0.0373	0.0349	0.0332	Mesophyll conductance	0.0081	0.0030	0.0034	0.0072	Post-photosynthesis	0.0247	0.0343	0.0315	0.0260
	50–60%		0.0367	0.0437	0.0382	0.0374		0.0018	0.0058	0.0094	0.0004		0.0349	0.0379	0.0288	0.0370
	60–70%		0.0405	0.0366	0.0421	0.0409		0.0018	0.0050	0.0026	0.0007		0.0387	0.0316	0.0395	0.0402
	70–80%		0.0444	0.0453	0.0413	0.0452		0.0044	0.0052	0.0103	0.0013		0.0400	0.0401	0.0310	0.0439
	100%		0.0441	0.0453	0.0456	0.0472		0.0057	0.0040	0.0025	0.0039		0.0384	0.0413	0.0431	0.0433
Q. variabilis	35–45%		0.0388	0.0402	0.0406	0.0384		0.0007	0.0025	0.0006	0.0091		0.0381	0.0377	0.0400	0.0293
	50–60%		0.0433	0.0448	0.0409	0.0368		0.0061	0.0084	0.0023	0.0018		0.0372	0.0364	0.0386	0.0350
	60–70%		0.0424	0.0440	0.0445	0.0414		0.0066	0.0086	0.0078	0.0041		0.0358	0.0354	0.0367	0.0373
	70–80%		0.0424	0.0446	0.0482	0.0457		0.0034	0.0016	0.0074	0.0028		0.0390	0.0430	0.0408	0.0429
	100%		0.0441	0.0466	0.0466	0.0398		0.0027	0.0076	0.0022	0.0125		0.0414	0.0390	0.0444	0.0273

654

Table

655 **Table 1.** Orthogonal treatments applied to *P. orientalis* and *Q. variabilis*.

P. orientalis	Repeats (cultivated period)	B_1	B_2	B_3	B_4	B_5
A_1	R_1:June 2–9	$A_1B_1R_1$	$A_1B_2R_1$	$A_1B_3R_1$	$A_1B_4R_1$	$A_1B_5R_1$
	R_2:June 12–19	$A_1B_1R_2$	$A_1B_2R_2$	$A_1B_3R_2$	$A_1B_4R_2$	$A_1B_5R_2$
A_2	R_1:July 11–18	$A_2B_1R_1$	$A_2B_2R_1$	$A_2B_3R_1$	$A_2B_4R_1$	$A_2B_5R_1$
	R_2:July 22–29	$A_2B_1R_2$	$A_2B_2R_2$	$A_2B_3R_2$	$A_2B_4R_2$	$A_2B_5R_2$
A_3	R_1:June 2–9	$A_3B_1R_1$	$A_3B_2R_1$	$A_3B_3R_1$	$A_3B_4R_1$	$A_3B_5R_1$
	R_2:June 12–19	A_3B_1R	$A_3B_2R_2$	$A_3B_3R_2$	$A_3B_4R_2$	$A_3B_5R_2$
A_4	R_1:July 11–18	$A_4B_1R_1$	$A_4B_2R_1$	$A_4B_3R_1$	$A_4B_4R_1$	$A_4B_5R_1$
	R_2:July 22–29	$A_4B_1R_2$	$A_4B_2R_2$	$A_4B_3R_2$	$A_4B_4R_2$	$A_4B_5R_2$
Q. variabilis	Repeats (cultivated period)	B_1	B_2	B_3	B_4	B_5
A_1	P_1:June 21–28	$A_1B_1P_1$	$A_1B_2P_1$	$A_1B_3P_1$	$A_1B_4P_1$	$A_1B_5R_1$
	P_2:July 2–9	$A_1B_1P_2$	$A_1B_2P_2$	$A_1B_3P_2$	$A_1B_4P_2$	$A_1B_5R_2$
A_2	P_1:August 4–11	$A_2B_1P_1$	$A_2B_2P_1$	$A_2B_3P_1$	$A_2B_4P_1$	$A_2B_5R_1$
	P_2:August 15–22	$A_2B_1P_2$	$A_2B_2P_2$	$A_2B_3P_2$	$A_2B_4P_2$	$A_2B_5R_2$
A_3	P_1:June 21–28	$A_3B_1P_1$	$A_3B_2P_1$	$A_3B_3P_1$	$A_3B_4P_1$	$A_3B_5R_1$
	P_2:July 2–9	$A_3B_1P_2$	$A_3B_2P_2$	$A_3B_3P_2$	$A_3B_4P_2$	$A_3B_5R_2$
A_4	P_1:August 4–11	$A_4B_1P_1$	$A_4B_2P_1$	$A_4B_3P_1$	$A_4B_4P_1$	$A_4B_5R_1$
	P_2:August 15–22	$A_4B_1P_2$	$A_4B_2P_2$	$A_4B_3P_2$	$A_4B_4P_2$	$A_4B_5R_2$

656